*Progress In Electromagnetics Research B, Vol. 80, 59–77, 2018*

# Cognitive Radar Waveform Design against Signal-Dependent Modulated Jamming

**Shuping Lu, Guolong Cui*, Xianxiang Yu, Lingjiang Kong, and Xiaobo Yang**

**Abstract**—This paper focuses on the cognitive design of transmit waveform to improve target detection capability in the presence of signal-dependent modulated jamming (e.g., chopping and interleaving (C&I) jamming). In particular, we reasonably assume that the modulation mode of signal-dependent jamming is available based on cognitive paradigm. The first design criterion is to minimize the integrated cross-correlation energy (ICE) between the transmit waveform and jamming signal. In this way, the received jamming signal can be suppressed after matched filter processing is performed using the optimized waveform. The second design criterion is to minimize the integrated auto-correlation sidelobe level (IASL) for maintaining good range compression property. The practical constant modulus constraint is imposed on the transmit waveform. Finally, to deal with the resulting non-convex problem, an iterative algorithm based on the majorization-minimization framework is developed. Numerical examples for specific signal-dependent modulated jammings are provided to demonstrate the effectiveness of the proposed methodology.

## 1. INTRODUCTION

Interference rejection is a long-standing issue in radar, sonar, communications, and other fields [1–3] since unwanted interferences contaminate echoes, shield useful information, and further cause false information. The forms of interferences are diversified and dynamic, including land and sea clutter, unintentional civil electromagnetic, hostile electronic jamming, etc. Some of them are related with transmit signals, namely signal-dependent interference [4]. Particularly, in electronic countermeasures (ECM), the jammer can generate a kind of signal-dependent modulated jamming which is specialized for deceiving radar receiver [5].

Waveform diversity technique has received considerable attention since it is proved to be an effective interference rejection way [6–8]. These works can be classified into two categories. The first category only focuses on the synthesis of transmit signal, in which the considered issues include shaped transmit beam pattern [9], the maximization of signal-to-interference-plus-noise ratio (SINR) or detection of probability [10, 11], good ambiguity function properties [12], etc. For instance, in [10], a waveform design method by maximizing SINR and accounting for similarity constraint is developed on the basis of the known covariance matrix of interference and noise. In [11], authors design a phase-only coding waveform by considering the maximization of detection of probability in the presence of signal-independent interference.

The second category addresses the waveform design problem by jointly optimizing transmitter-receiver design [13]. Specifically, in [14, 15], the transmit waveform and receive filter are jointly devised for the detection and classification problem of extended target. In [16], several CREW (Cognitive REceiver and Waveform design) optimization methods are proposed so as to minimize the mean-square

*Received 8 January 2018, Accepted 26 February 2018, Scheduled 17 March 2018*

* Corresponding author: Guolong Cui (cuiguolong@uestc.edu.cn).

The authors are with the School of Information and Communication Engineering, University of Electronic Science and Technology of China, Chengdu, Sichuan, P. R. China.

error (MSE) of target backscattering coefficient estimate in signal-dependent clutter environment. By exploiting a dynamic environmental database including clutter maps, spectral clutter models, etc., the cognitive transmit signal with constant modulus and similarity constraints and the mismatched receive filter are devised to maximize the output SINR [17]. For a co-located multiple-input and multiple-output (MIMO) radar system, two sequential optimization algorithms are proposed to jointly design the transmit waveform under constant modulus and similarity constraints and the receive filter embedded in signal-dependent interference plus white gaussian noise [18]. In [19], through a max-min convex optimization approach, the SINR considered as the figure of merit is maximized with the aim of jointly designing waveform covariance matrix and filter for airborne MIMO system in the presence of clutter and jamming.

It is worth observing that most aforementioned works focus on dealing with the interference returning from high reverberating environment. However, the research on suppressing the signal-dependent modulated jamming through waveform optimization has hardly been considered in open literature. This type of interference is common in ECM. The digital radio frequency memory (DRFM) can intercept and repeat the radar signal to generate signal-dependent modulated jamming, such as chopping and interleaving (C&I) jamming signal [20], which results in some false peaks in other neighboring range cells to deceive radar receiver.

In this paper, we investigate the phase-only coding waveform design in the presence of signal-dependent modulated jamming, by taking into account the matched-filter case. In [21], a dynamic environment database based on the idea of cognitive radar is builded to provide the *a priori* information for knowledge-aided operation. Furthermore, in [22], an electronic support measurement (ESM) system is employed to acquire the information concerning hostile jammer. More specifically, we assume that the modulation parameters of signal-dependent modulated jamming can be obtained under cognitive paradigm. Then we present two waveform design criterions based on the matched filter processing. The first one is to reduce the integrated cross-correlation energy (ICE) between the transmit signal and the jamming signal for jamming rejection. In the second criterion, the integrated auto-correlation sidelobe level (IASL) of the transmit waveform is minimized for maintaining good range compression property [23]. In practical radar applications, the constant modulus constraint is often considered in waveform design because of the maximum clipping effect of the power amplifiers and A/D converters [16]. By exploiting the two design criterions, we formulate a non-convex and constrained optimization problem. Then resorting to the majorization-minimization (MM) simplification [24], we propose a novel iteration algorithm to solve it. In each iteration, we develop the multi-dimensional problem into an one-dimension problem with closed-form solution. The computational complexity is linear in the number of iterations and polynomial in the size of designed waveform. Finally, we evaluate the capability of the proposed algorithm through numerical simulations considering the C&I and smeared spectrum (SMSP) distance deception jammings, which are typical signal-dependent modulated jammings.

The rest of the paper is organized as follows. In Section 2, we introduce the waveform design criterions and formulate the optimization problem. In Section 3, we present an iterative algorithm to solve the optimization problem. In Section 4, we evaluate the proposed methodology by numerical examples. Finally, in Section 5, we give a brief conclusion and possible future research tracks.

*Notation*: In the sequel, vectors and matrices are denoted by boldface lower case ($\boldsymbol{a}$) and upper case ($\boldsymbol{A}$) letters, respectively. The $n$-th element of $\boldsymbol{a}$ is denoted by $a_n$. The $\boldsymbol{a}^{(n)}$ denotes the $n$-th iterative result of $\boldsymbol{a}$. Superscripts $\mathrm{Tr}(\cdot)$, $(\cdot)^T$, $(\cdot)^*$, and $(\cdot)^\dagger$ denote the trace, transpose, complex conjugate, and complex conjugate transpose, respectively. The letter $j$ represents the imaginary unit (i.e., $j=\sqrt{-1}$). $\Re e(x)$ and $\mathrm{Arg}(x)$ are the real part and the argument of a complex number $x$, respectively. $\mathrm{vec}(\boldsymbol{A})$ is a column vector of orderly arraying all the columns of $\boldsymbol{A}$. As to the numerical sets, $\mathbb{C}$ is the set of complex numbers, and $\mathbb{C}^{N\times M}$ is the Euclidean space of $(N\times M)$-dimensional complex matrices (or vectors if $M=1$). $\boldsymbol{I}_N$ stands for the $N\times N$ identity matrix. $\boldsymbol{1}_N$ is the $N$-dimensional vector where every element is equal to 1. $\min\limits_{x} f(x)$ denotes the minimizing operation on the function $f(x)$ with respect to $x$. The abbreviation "s.t." stands for "subject to".

## 2. PROBLEM FORMULATION

We consider a monostatic radar system which transmits an intrapluse phase-coded sequence $\boldsymbol{s} = [s_1, s_2, \ldots, s_N]^T \in \mathbb{C}^{N\times 1}$. More precisely, taking account of constant modulus constraint and normalized transmitted energy, the element of $\boldsymbol{s}$ can be given by

$$s_n = \frac{1}{\sqrt{N}} e^{j\phi_n}, \quad n = 1, \ldots, N \tag{1}$$

with $\phi_n \in [0, 2\pi)$ being the phase of $s_n$.

In ECM system, the jammer using DRFM can intercept, repeat, and modulate the radar transmit waveform to produce signal-dependent modulated jamming. It is retransmitted towards the radar and deceives radar receiver by producing many false targets. According to the modulation mechanism of the representative signal-dependent modulated jamming[†], we establish the following jamming signal model

$$\boldsymbol{c} = \boldsymbol{J}_c \boldsymbol{s} \in \mathbb{C}^{N\times 1}, \quad \boldsymbol{J}_c \neq \alpha \boldsymbol{I}_N \tag{2}$$

where $\boldsymbol{J}_c$ and $\alpha$ denote the jamming shifting matrix and a positive real number, respectively. Namely, there is a linear correlation between the jamming signal and the transmit waveform. In this paper, it is worth pointing out that there is a limitation $\boldsymbol{J}_c \neq \alpha \boldsymbol{I}_N$. In other words, the signal-dependent modulated jamming model $\boldsymbol{c}$ does not include the complete repeater jamming[‡]. Furthermore, we assume that $\boldsymbol{J}_c$ is known based on cognitive paradigm. Some preprocessing frontiers or memory segments in cognitive system can obtain the *a priori* information and experience data about radar environment [25]. In fact, there have been some studies on the classification and feature extraction of jamming signal [26, 27]. For instance, in [28], a matched signal transform algorithm was introduced to identify the SMSP jamming type. In [29], authors utilized time-frequency analysis to estimate the parameters of the C&I jamming.

The radar receiver implements the matched-filter processing after receiving the echo signal consisting of target scattering and jamming. In order to eliminate the jamming effect, we expect that the correlation energy between the jamming signal and transmit waveform can be minimized. Meanwhile, the IASL is also suppressed to avoid the potential range sidelobe interference. Herein, as low as possible ICE between $\boldsymbol{c}$ and $\boldsymbol{s}$ and IASL of $\boldsymbol{s}$ should be achieved. We give the following proposition to compute the ICE and IASL.

**Proposition 2.1.** *The ICE and IASL functions with the known $\boldsymbol{J}_c$ are given by*

$$\mathrm{ICE}(\boldsymbol{s}) = \sum_{k=1}^{N-1} \left| \boldsymbol{s}^\dagger \boldsymbol{J}_k^T \boldsymbol{J}_c \boldsymbol{s} \right|^2 + \sum_{k=0}^{N-1} \left| \boldsymbol{s}^\dagger \boldsymbol{J}_k \boldsymbol{J}_c \boldsymbol{s} \right|^2, \tag{3}$$

*and*

$$\mathrm{IASL}(\boldsymbol{s}) = 2 \sum_{k=1}^{N-1} \left| \boldsymbol{s}^\dagger \boldsymbol{J}_k \boldsymbol{s} \right|^2, \tag{4}$$

*respectively, where $\boldsymbol{J}_k$, $k = 0, 1, \ldots, N-1$ is a defined shifting matrix as specified in Appendix B and satisfies $\boldsymbol{J}_k = \boldsymbol{J}_{-k}^\dagger$.*

*Proof.* See Appendix B.

It is worth pointing out that the simultaneous minimization of both ICE and IASL is hard in the whole range cells. However, it would be easier to suppress these sidelobe levels located at some range cells of interest. To this end, two weight vectors $\boldsymbol{w}_1 = [w_{1,1}, \ldots, w_{1,2N-1}]^T \in [0, 1]$, and $\boldsymbol{w}_2 = [w_{2,1}, \ldots, w_{2,N-1}]^T \in [0, 1]$ are provided so as to flexibly control the sidelobe levels of ICE and IASL, respectively. The optimization problem considering weights $\boldsymbol{w}_1$ and $\boldsymbol{w}_2$ can be expressed as

$$\begin{aligned} \min_{\boldsymbol{s}} \quad & \mathrm{ICE}(\boldsymbol{s}, \boldsymbol{w}_1),\ \mathrm{IASL}(\boldsymbol{s}, \boldsymbol{w}_2) \\ \text{s.t.} \quad & |s_n| = \frac{1}{\sqrt{N}}, \quad n = 1, \ldots, N. \end{aligned} \tag{5}$$

[†] The modulation mechanisms of the C&I and SMSP jammings are illustrated in Appendix A

[‡] To be exact, the following design criterion of lowering the cross-correlation level between the jamming signal $\boldsymbol{c}$ and transmitted waveform $\boldsymbol{s}$ does not apply when $\boldsymbol{c} = \alpha \boldsymbol{s}$.

In general, a feasible solution that minimizes all the objective functions simultaneously is nearly nonexistent for the above multi-objective optimization problem. Herein, based on the scalarization technique [30], we set a factor $\lambda \in [0,1]$ as a trade-off between ICE$(\boldsymbol{s},\boldsymbol{w}_1)$ and IASL$(\boldsymbol{s},\boldsymbol{w}_2)$, and then obtain one or more Pareto-optimal solutions. Accordingly, the parameterized optimization multi-objective function is defined as

$$\mathrm{W}\boldsymbol{\Lambda}(\boldsymbol{s},\lambda,\boldsymbol{w}_1,\boldsymbol{w}_2) = \mathrm{WICE}(\boldsymbol{s},\lambda,\boldsymbol{w}_1) + \mathrm{WIASL}(\boldsymbol{s},\lambda,\boldsymbol{w}_2) \tag{6}$$

where

$$\begin{cases} \mathrm{WICE}(\boldsymbol{s},\lambda,\boldsymbol{w}_1) = \lambda\left(\sum\limits_{k=1}^{N-1} w_{1,N-k}\left|\boldsymbol{s}^\dagger \boldsymbol{J}_k^T \boldsymbol{J}_c \boldsymbol{s}\right|^2 + \sum\limits_{k=0}^{N-1} w_{1,N+k}\left|\boldsymbol{s}^\dagger \boldsymbol{J}_k \boldsymbol{J}_c \boldsymbol{s}\right|^2\right), \\ \mathrm{WIASL}(\boldsymbol{s},\lambda,\boldsymbol{w}_2) = 2(1-\lambda)\sum\limits_{k=1}^{N-1} w_{2,k}\left|\boldsymbol{s}^\dagger \boldsymbol{J}_k \boldsymbol{s}\right|^2. \end{cases} \tag{7}$$

Based on the aforementioned discussions, the waveform design about the suppression of signal-dependent modulated jamming and range sidelobe levels with constant modulus constraint can be formulated in terms of the following optimization problem

$$P_{\boldsymbol{s}} \begin{cases} \min_{\boldsymbol{s}} & \mathrm{W}\boldsymbol{\Lambda}(\boldsymbol{s},\lambda,\boldsymbol{w}_1,\boldsymbol{w}_2) \\ \text{s.t.} & |s_n| = \dfrac{1}{\sqrt{N}}, \quad n = 1,\ldots,N. \end{cases}$$

If $\lambda = 1$ and $\boldsymbol{w}_1 = \boldsymbol{1}_{2N-1}$, $P_{\boldsymbol{s}}$ only carries out ICE$(\boldsymbol{s})$ minimization. Problem $P_{\boldsymbol{s}}$ is a non-convex constrained problem and NP-hard [31]. In general, it is hard to get an analytical solution due to the non-convex constrained feasible set.

## 3. ITERATIVE OPTIMIZATION ALGORITHM

In the following, we propose an iterative search algorithm to tackle Problem $P_{\boldsymbol{s}}$, which includes two steps. First, we simplify the fourth power of the probing waveform problem to the second power using MM outside iteration. Second, we deal with the quadratic form based on an inside iterative search approach.

### 3.1. Step 1: Outside Iterative Optimization

In terms of Eq. (7), WICE$(\boldsymbol{s},\lambda,\boldsymbol{w}_1)$ can be recast as

$$\begin{aligned} \mathrm{WICE}(\boldsymbol{s},\lambda,\boldsymbol{w}_1) &= \lambda\left(\sum_{k=1}^{N-1} w_{1,N-k}\boldsymbol{s}^\dagger \boldsymbol{J}_k^T \boldsymbol{J}_c \boldsymbol{s}\boldsymbol{s}^\dagger \boldsymbol{J}_c^\dagger \boldsymbol{J}_k \boldsymbol{s} + \sum_{k=0}^{N-1} w_{1,N+k}\boldsymbol{s}^\dagger \boldsymbol{J}_k \boldsymbol{J}_c \boldsymbol{s}\boldsymbol{s}^\dagger \boldsymbol{J}_c^\dagger \boldsymbol{J}_k^T \boldsymbol{s}\right) \\ &= \boldsymbol{s}^\dagger\left[\lambda\sum_{k=1}^{N-1}\left(w_{1,N-k}\boldsymbol{J}_k^T \boldsymbol{J}_c \boldsymbol{s}\boldsymbol{s}^\dagger \boldsymbol{J}_c^\dagger \boldsymbol{J}_k + w_{1,N+k}\boldsymbol{J}_k \boldsymbol{J}_c \boldsymbol{s}\boldsymbol{s}^\dagger \boldsymbol{J}_c^\dagger \boldsymbol{J}_k^T\right) + \lambda w_{1,N}\boldsymbol{J}_c \boldsymbol{s}\boldsymbol{s}^\dagger \boldsymbol{J}_c^\dagger\right]\boldsymbol{s}. \end{aligned} \tag{8}$$

Using the similar process as Eq. (8), we can get

$$\mathrm{W}\boldsymbol{\Lambda}(\boldsymbol{s},\lambda,\boldsymbol{w}_1,\boldsymbol{w}_2) = \boldsymbol{s}^\dagger \boldsymbol{\Phi}(\boldsymbol{s})\boldsymbol{s} \tag{9}$$

where

$$\begin{aligned} \boldsymbol{\Phi}(\boldsymbol{s}) = \sum_{k=1}^{N-1}\Bigg[&2(1-\lambda)w_{2,k}\boldsymbol{J}_k \boldsymbol{s}\boldsymbol{s}^\dagger \boldsymbol{J}_k^T + \lambda\Big(w_{1,N-k}\boldsymbol{J}_k^T \boldsymbol{J}_c \boldsymbol{s}\boldsymbol{s}^\dagger \boldsymbol{J}_c^\dagger \boldsymbol{J}_k \\ &+ w_{1,N+k}\boldsymbol{J}_k \boldsymbol{J}_c \boldsymbol{s}\boldsymbol{s}^\dagger \boldsymbol{J}_c^\dagger \boldsymbol{J}_k^T\Big)\Bigg] + \lambda w_{1,N}\boldsymbol{J}_c \boldsymbol{s}\boldsymbol{s}^\dagger \boldsymbol{J}_c^\dagger. \end{aligned} \tag{10}$$

Apparently, Eq. (9) is still the fourth power of the transmit waveform. In [18], two sequential iterative optimization algorithms were developed to solve the similar optimization form $\boldsymbol{s}^\dagger \boldsymbol{\Phi}(\boldsymbol{s})\boldsymbol{s}$, but

which cannot ensure the monotonicity and convergence for Problem $P_{\boldsymbol{s}}$ from a theoretical point of view. Interestingly, some papers such as [11, 16, 32] have investigated the maximization of the quadratic expression $\boldsymbol{s}^{\dagger}\boldsymbol{\Phi}\boldsymbol{s}$ with $\boldsymbol{\Phi}$ being independent of $\boldsymbol{s}$, where the convergence can be ensured. In order to guarantee these considered properties, we resort to the framework of the MM algorithm [33]. In the following, we provide a proposition to simplify Problem $P_{\boldsymbol{s}}$ into a similar quadratic expression.

**Proposition 3.1.** *Let $\{\boldsymbol{s}^{(m+1)}\}_{m=0}^{\infty}$ be a sequence of constant modular codes. Then Problem $P_{\boldsymbol{s}}$ can be transformed into an iterative constant-modulus quadratic program (ICQP) problem:*

$$P_{\boldsymbol{s}^{(m+1)}} \begin{cases} \min_{\boldsymbol{s}^{(m+1)}} & \left(\boldsymbol{s}^{(m+1)}\right)^{\dagger} \boldsymbol{\Upsilon}\left(\boldsymbol{s}^{(m)}\right) \boldsymbol{s}^{(m+1)} \\ \text{s.t.} & s_n^{(m+1)} = \dfrac{1}{\sqrt{N}} e^{j\phi_n} \\ & \phi_n \in [0, 2\pi), \quad n = 1, \ldots, N \end{cases}$$

*where*

$$\Upsilon\left(\boldsymbol{s}^{(m)}\right) = \frac{\boldsymbol{G}^{\dagger}\left(\boldsymbol{s}^{(m)}\right) + \boldsymbol{G}\left(\boldsymbol{s}^{(m)}\right)}{2}, \tag{11}$$

*while $\boldsymbol{G}(\boldsymbol{s}^{(m)})$ is given by Eq. (C7).*

*Proof.* See Appendix C.

In **Proposition 3.1**, we cast the minimization function $\boldsymbol{s}^{\dagger}\boldsymbol{\Phi}(\boldsymbol{s})\boldsymbol{s}$ into an ICQP problem where $\boldsymbol{\Upsilon}(\boldsymbol{s}^{(m)})$ is tantamount to a constant for $\boldsymbol{s}^{(m+1)}$ of the $(m+1)$th iteration. In other words, we implement an order reduction transformation by the outside iteration optimization.

In order to satisfy the principle that the minimization of objective function is equivalent to the minimization of majorization function [24], we must construct a majorization function for Eq. (9). In the proof of **Proposition 3.1**, $u_1(\boldsymbol{S}, \boldsymbol{S}^{(m)})$, namely Eq. (C3), is the constructed majorization function of $\boldsymbol{s}^{\dagger}\boldsymbol{\Phi}(\boldsymbol{s})\boldsymbol{s}$ where $\boldsymbol{\Phi}(\boldsymbol{s})$ is a Hermitian matrix. Meanwhile, in each iteration, the following formula can be satisfied

$$\left(\boldsymbol{s}^{(m+1)}\right)^{\dagger} \boldsymbol{\Phi}\left(\boldsymbol{s}^{(m+1)}\right) \boldsymbol{s}^{(m+1)} \leq u_1\left(\boldsymbol{S}^{(m+1)}, \boldsymbol{S}^{(m)}\right) \leq u_1\left(\boldsymbol{S}^{(m)}, \boldsymbol{S}^{(m)}\right) = \left(\boldsymbol{s}^{(m)}\right)^{\dagger} \boldsymbol{\Phi}\left(\boldsymbol{s}^{(m)}\right) \boldsymbol{s}^{(m)} \tag{12}$$

where $\boldsymbol{S} = \boldsymbol{s}\boldsymbol{s}^{\dagger}$, and the iteration of $u_1(\boldsymbol{S}^{(m+1)}, \boldsymbol{S}^{(m)})$ is equivalent to the minimization of the objective function of Problem $P_{\boldsymbol{s}^{(m+1)}}$. Hence, Eq. (12) can ensure that the objective value $\boldsymbol{s}^{\dagger}\boldsymbol{\Phi}(\boldsymbol{s})\boldsymbol{s}$ monotonically decreases during the outside iterative procedure. More details about the MM method can be found in [33, 34].

### 3.2. Step 2: Inside Iterative Optimization

The second step focuses on the solution of Problem $P_{\boldsymbol{s}^{(m+1)}}$. We introduce an iterative search (IS) algorithm, which can be efficiently used to solve the quadratic problem $\boldsymbol{s}^{\dagger}\boldsymbol{\Phi}\boldsymbol{s}$ under constant modulus constraint. The principle of this method is to sequentially optimize $\boldsymbol{s}$ over one variable keeping the others fixed, namely alternate optimization. Firstly, we recast the minimization of $(\boldsymbol{s}^{(m+1)})^{\dagger}\boldsymbol{\Upsilon}(\boldsymbol{s}^{(m)})\boldsymbol{s}^{(m+1)}$ as the maximization of $(\boldsymbol{s}^{(m+1)})^{\dagger}(-\boldsymbol{\Upsilon}(\boldsymbol{s}^{(m)}))\boldsymbol{s}^{(m+1)}$. Let $\{\boldsymbol{s}^{(i+1)}\}_{i=0}^{\infty}$ be a sequence of constant modular codes, where $i$ denotes the inside iteration number. Problem $P_{\boldsymbol{s}^{(m+1)}}$ can be rewritten as

$$P_{s_n^{(i+1)}} \begin{cases} \max_{\boldsymbol{s}^{(i+1)}} & \left(\boldsymbol{s}^{(i+1)}\right)^{\dagger} \left(-\boldsymbol{\Upsilon}\left(\boldsymbol{s}^{(m)}\right)\right) \boldsymbol{s}^{(i+1)} \\ \text{s.t.} & s_n^{(i+1)} = \dfrac{1}{\sqrt{N}} e^{j\phi_n} \\ & \phi_n \in [0, 2\pi), \ n = 1, \ldots, N \end{cases}$$

where $\boldsymbol{s}^{(i+1)} = [s_1^{(i+1)}, \ldots, s_n^{(i+1)}, \ldots, s_N^{(i+1)}]^T$. In the $(i+1)$th inside iteration, we sequentially optimize each code element of $\boldsymbol{s}^{(i+1)}$ and fix the remaining $N-1$ code elements. Let $\overline{\boldsymbol{s}}^{(i+1)} = \boldsymbol{s}^{(i)}$. For the optimization of the $n$th element, let $\overline{s}_n^{(i+1)} = 0$, and then the new solution is given by

$$\overline{s}_n^{(i+1)} = \frac{1}{\sqrt{N}} e^{j\mathrm{Arg}\left(-\boldsymbol{\Upsilon}(:,n)^{\dagger}\left(\overline{\boldsymbol{s}}^{(i+1)}\right)^{*}\right)}. \tag{13}$$

The IS processing of single variable turns the whole $N$-dimensional search problem into one dimension. The detailed discussion about the inside IS algorithm can be found in [35]. We call the MM framework plus IS method "MM-IS", which is summarized in **Algorithm 1**.

**Algorithm 1** : MM-IS Algorithm for solving $P_{\boldsymbol{s}}$

**Require:** $N$, $\lambda$, $\boldsymbol{w}_1$, $\boldsymbol{w}_2$, $\delta_1$, $\delta_2$, and $\boldsymbol{J}_c$, where $\delta_1$ and $\delta_2$ are small positive real numbers;
**Ensure:** An optimal solution $\boldsymbol{s}^\star$ to Problem $P_{\boldsymbol{s}}$;

1: Compute $\boldsymbol{J}_k, k = 0, 1, \ldots, N$ by Eq. (B2), the matrix $\boldsymbol{\Psi}$ by Eq. (C2), and the maximum eigenvalue $\lambda_{\max}$ of $\boldsymbol{\Psi}$;
2: Let $m = 0$;
3: Randomly initialize the phase sequence $\boldsymbol{\phi}^{(0)}$ over the interval $[0, 2\pi)$. Then the initial constant modulus sequence can be written as $\boldsymbol{s}^{(0)} = \frac{1}{\sqrt{N}} e^{j\boldsymbol{\phi}^{(0)}}$;
4: Compute $\boldsymbol{\Upsilon}\left(\boldsymbol{s}^{(0)}\right) = \frac{\boldsymbol{G}^\dagger\left(\boldsymbol{s}^{(0)}\right) + \boldsymbol{G}\left(\boldsymbol{s}^{(0)}\right)}{2}$ by Eq. (C7) and $\mathrm{W}\boldsymbol{\Lambda}\left(\boldsymbol{s}^{(0)}\right) = \left(\boldsymbol{s}^{(0)}\right)^\dagger \boldsymbol{\Phi}\left(\boldsymbol{s}^{(0)}\right) \boldsymbol{s}^{(0)}$ by Eq. (9);
5: $m = m + 1$;
6: Let $i = 0$, $\overline{\boldsymbol{s}}^{(i)} = \boldsymbol{s}^{(m-1)}$ and $\rho_0 = \left(\boldsymbol{s}^{(i)}\right)^\dagger \left(-\boldsymbol{\Upsilon}\left(\boldsymbol{s}^{(m-1)}\right)\right) \boldsymbol{s}^{(i)}$;
7: $i = i + 1$, $n = 1$, $\overline{\boldsymbol{s}}^{(i)} = \boldsymbol{s}^{(i-1)}$;
8: Let $\overline{s}_n^{(i)} = 0$, then $\overline{s}_n^{(i)} = \frac{1}{\sqrt{N}} \exp\left(j \mathrm{Arg}\left(\boldsymbol{\Upsilon}(:, n)^\dagger \left(\overline{\boldsymbol{s}}^{(i)}\right)^*\right)\right)$;
9: $n = n + 1$; If $n = N + 1$, go to next step; Otherwise, return to step 8;
10: Let $\boldsymbol{s}^{(i)} = \overline{\boldsymbol{s}}^{(i)}$, and compute $\rho_i$.
11: If $|\rho_i - \rho_{i-1}| < \delta_1$, where $\delta_1$ is a parameter to control inside convergence, go to next step; Otherwise, return to step 7;
12: Let $\boldsymbol{s}^{(m)} = \boldsymbol{s}^{(i)}$, and compute $\mathrm{W}\boldsymbol{\Lambda}\left(\boldsymbol{s}^{(m)}\right)$;
13: If $\frac{\left|\mathrm{W}\boldsymbol{\Lambda}\left(\boldsymbol{s}^{(m)}\right) - \mathrm{W}\boldsymbol{\Lambda}\left(\boldsymbol{s}^{(m-1)}\right)\right|}{\mathrm{W}\boldsymbol{\Lambda}\left(\boldsymbol{s}^{(m-1)}\right)} < \delta_2$, where $\delta_2$ is a parameter to control outside convergence, output $\boldsymbol{s}^\star = \boldsymbol{s}^{(m)}$; Otherwise, compute $\boldsymbol{\Upsilon}\left(\boldsymbol{s}^{(m)}\right)$, and return to step 5.

*Remark:* As previously mentioned, some existing optimization algorithms are aimed at Problem $P_{\boldsymbol{s}^{(m+1)}}$ to solve $\boldsymbol{s}^{(m+1)}$. According to [11], we can relax $(\boldsymbol{s}^{(m+1)})^\dagger \boldsymbol{\Upsilon}(\boldsymbol{s}^{(m)}) \boldsymbol{s}^{(m+1)}$ by using Semi-Definite Relaxation (SDP) without considering rank-one and constant modulus constraints and further synthesize code by using random approach. However, this method costs a huge computation burden especially for the large size of $\boldsymbol{s}$. Additionally, this method also requires a reasonable choice of the number of random trials. Besides, in [32], a power method like iterative approach was introduced to solve unimodular quadratic program problem. Moreover, since $\boldsymbol{\Upsilon}(\boldsymbol{s}^{(m)})$ is positive definite and a Hermitian matrix, another feasible optimization method is to use the MM simplification again. The quadratic program problem can be recast as one power of $\boldsymbol{s}$.

## 4. NUMERICAL EXAMPLES

We analyze and evaluate the performance of the proposed waveform design algorithm via numerical simulations. The C&I and SMSP distance deception jammings are employed as specific signal-dependent modulated jamming examples. Their modulation forms and corresponding shifting matrixes are shown in Appendix A and assumed to be known. For simplicity, we only use C&I jamming in Subsections 4.1 $\sim$ 4.3. The C&I jamming parameter $p$ is fixed to 16 (It has little impact on the experimental conclusions). In the last subsection, we employ both the jamming forms to analyze the matched-filter performance. If not otherwise stated, the weights are set to $\boldsymbol{w}_1 = \boldsymbol{1}_{2N-1}$, $\boldsymbol{w}_2 = \boldsymbol{1}_{N-1}$, and $\lambda = 0.5$.

In [24], an algorithm utilizing twice MM processes was introduced for designing sequences with low autocorrelation sidelobes. We apply the idea of the algorithm to solving Problem $P_{\boldsymbol{s}^{(m+1)}}$. To further simply the objective function of $P_{\boldsymbol{s}^{(m+1)}}$, let $\boldsymbol{Q} = \eta 2 \boldsymbol{I}_N$, where $\eta 2$ is the maximum eigenvalue of $\boldsymbol{\Upsilon}(\boldsymbol{s}^{(m)})$.

Then the majorization function $u2$ of $(\boldsymbol{s}^{(m+1)})^{\dagger}\boldsymbol{\Upsilon}(\boldsymbol{s}^{(m)})\boldsymbol{s}^{(m+1)}$ can be expressed as

$$\begin{aligned} u2\left(\boldsymbol{s}^{(m+1)},\boldsymbol{s}^{(m)}\right) &= \left(\boldsymbol{s}^{(m+1)}\right)^{\dagger}\boldsymbol{Q}\boldsymbol{s}^{(m+1)} + \left(\boldsymbol{s}^{(m)}\right)^{\dagger}\left(\boldsymbol{Q}-\boldsymbol{\Upsilon}(\boldsymbol{s}^{(m)})\right)\boldsymbol{s}^{(m)} \\ &\quad +2\Re e\left(\left(\boldsymbol{s}^{(m+1)}\right)^{\dagger}\left(\boldsymbol{\Upsilon}\left(\boldsymbol{s}^{(m)}\right)-\boldsymbol{Q}\right)\boldsymbol{s}^{(m)}\right). \end{aligned} \tag{14}$$

The first two items of $u2(\boldsymbol{s}^{(m+1)},\boldsymbol{s}^{(m)})$ are constant because $(\boldsymbol{s}^{(m+1)})^{\dagger}\boldsymbol{s}^{(m+1)}=1$. We only need to tackle the last term. Let $\{\boldsymbol{s}^{(t+1)}\}_{t=0}^{\infty}$ be a sequence of constant modular codes, where $t$ denotes the inside iteration number. Problem $P_{\boldsymbol{s}^{(m+1)}}$ can be resolved into

$$P_{\boldsymbol{s}^{(t+1)}}\begin{cases} \min_{\boldsymbol{s}^{(t+1)}} & \left\|\boldsymbol{s}^{(t+1)}-\left(\boldsymbol{\Upsilon}\left(\boldsymbol{s}^{(m)}\right)-\boldsymbol{Q}\right)\boldsymbol{s}^{(m)}\right\|_2 \\ \text{s.t.} & s_n^{(t+1)}=\dfrac{1}{\sqrt{N}}e^{j\phi_n} \\ & \phi_n\in[0,2\pi),\ n=1,\ldots,N. \end{cases} \tag{15}$$

The closed-form solution of $P_{\boldsymbol{s}^{(t+1)}}$ is given by

$$\boldsymbol{s}^{(t+1)}=\frac{1}{\sqrt{N}}e^{j\mathrm{Arg}\left(\left(\boldsymbol{\Upsilon}(\boldsymbol{s}^{(m)})-\boldsymbol{Q}\right)\boldsymbol{s}^{(m)}\right)}. \tag{16}$$

Moreover, an acceleration via fixed point theory is applied to accelerate the iteration speed in [24]. We call the accelerated algorithm based on twice MM optimizations the MM-MM-Acc, which is summarized in **Algorithm** 2 for subsequent comparison.

**Algorithm 2** : MM-MM-Acc Algorithm for solving $P_{\boldsymbol{s}}$

**Require:** $\boldsymbol{w}_1$, $\boldsymbol{w}_2$, $\lambda$, $N$, $\delta$, and $\boldsymbol{J}_c$, where $\delta$ is a small positive real number;
**Ensure:** An optimal solution $\boldsymbol{s}^{\star}$ to $P_{\boldsymbol{s}}$;

1: Compute $\boldsymbol{J}_k, k=0,1,\ldots,N$ by Eq. (B2), and the maximum eigenvalue $\lambda_{\max}$ by Eq. (C2);
2: Let $m=0$;
3: Randomly initialize $\boldsymbol{s}^{(0)}$ over the interval $[0,2\pi)$ according to Eq. (1);
4: Compute $\Upsilon\left(\boldsymbol{s}^{(0)}\right)=\frac{\boldsymbol{G}^{\dagger}\left(\boldsymbol{s}^{(0)}\right)+\boldsymbol{G}\left(\boldsymbol{s}^{(0)}\right)}{2}$ by Eq. (C7), the maximum eigenvalue $\eta_2$ of $\Upsilon\left(\boldsymbol{s}^{(0)}\right)$, and $\mathrm{W}\boldsymbol{\Lambda}\left(\boldsymbol{s}^{(0)}\right)=\left(\boldsymbol{s}^{(0)}\right)^{\dagger}\boldsymbol{\Phi}\left(\boldsymbol{s}^{(0)}\right)\boldsymbol{s}^{(0)}$ by Eq. (9);
5: $m=m+1$;
6: Compute $\boldsymbol{x}1=\frac{1}{\sqrt{N}}e^{j\mathrm{Arg}\left(\left(\boldsymbol{\Upsilon}\left(\boldsymbol{s}^{(m-1)}\right)-\eta_2\boldsymbol{I}_N\right)\boldsymbol{s}^{(m-1)}\right)}$;
7: Compute $\mathrm{x}2=\frac{1}{\sqrt{N}}e^{j\mathrm{Arg}\left(\left(\boldsymbol{\Upsilon}\left(\boldsymbol{s}^{(m-1)}\right)-\eta_2\boldsymbol{I}_N\right)\boldsymbol{x}1\right)}$;
8: $\boldsymbol{x}_3=\boldsymbol{x}_1-\boldsymbol{s}^{(m-1)}$;
9: $\boldsymbol{x}_4=\boldsymbol{x}_2-\boldsymbol{x}_1-\boldsymbol{x}_3$;
10: Compute the step-length $\mathrm{L}=-\frac{\|\boldsymbol{x}_3\|}{\|\boldsymbol{x}_4\|}$;
11: Compute $\boldsymbol{s}^{(m)}=\frac{1}{\sqrt{N}}e^{j\mathrm{Arg}(\boldsymbol{s}^{(m-1)}-2\mathrm{L}\boldsymbol{x}_3+\mathrm{L}^2\boldsymbol{x}_4)}$;
12: Compute $\mathrm{W}\boldsymbol{\Lambda}\left(\boldsymbol{s}^{(m)}\right)=\left(\boldsymbol{s}^{(m)}\right)^{\dagger}\boldsymbol{\Phi}\left(\boldsymbol{s}^{(m)}\right)\boldsymbol{s}^{(m)}$;
13: If $\mathrm{W}\boldsymbol{\Lambda}\left(\boldsymbol{s}^{(m)}\right)>\mathrm{W}\boldsymbol{\Lambda}\left(\boldsymbol{s}^{(m-1)}\right)$, go to next step; Otherwise, go to step 15;
14: Recalculate the step-length $\mathrm{L}=(\mathrm{L}-1)/2$, return to step 11;
15: If $\frac{\left|\mathrm{W}\boldsymbol{\Lambda}\left(\boldsymbol{s}^{(m)}\right)-\mathrm{W}\boldsymbol{\Lambda}\left(\boldsymbol{s}^{(m-1)}\right)\right|}{\mathrm{W}\boldsymbol{\Lambda}\left(\boldsymbol{s}^{(m-1)}\right)}<\delta$, where $\delta$ is a parameter to control outside convergence, output $\boldsymbol{s}^{\star}=\boldsymbol{s}^{(m)}$; Otherwise, compute $\Upsilon\left(\boldsymbol{s}^{(m)}\right)$ and the maximum eigenvalue $\eta_2$ of $\boldsymbol{\Upsilon}\left(\boldsymbol{s}^{(m)}\right)$, and return to step 5.

### 4.1. Iteration Convergence Property

In this subsection, we investigate the iteration convergence feature of the objective function in Eq. (9). The sequence lengths are set to $N=32,64,128$. In Fig. 1, the normalized objective function versus

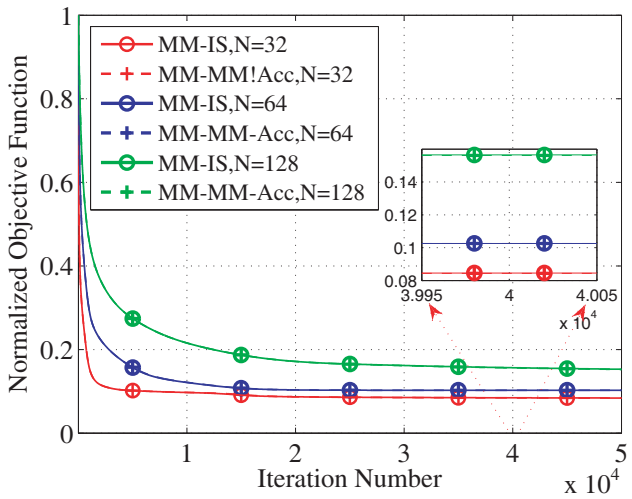


**Figure 1.** Iteration convergence curves of objective functions of MM-IS and MM-MM-Acc algorithms.

**Table 1.** Average running time (ms) of one outside iteration versus different algorithms and sequence lengths.

| Algorithm \ N | 32 | 64 | 128 |
|---|---|---|---|
| MM-IS | 13.9 | 28.6 | 99.8 |
| MM-MM-Acc | 14.3 | 29.6 | 103.3 |

iteration number is plotted. It is observed that all the function curves decrease monotonously as the iteration number increases. Besides, the convergence speed of the smaller sequence length is faster. Meanwhile, the iteration convergence trends of the MM-IS and MM-MM-Acc algorithms are basically the same. In other words, both iteration algorithms are strictly dominated by the MM framework of the outside iteration. Table 1 presents the running time of one iteration of both the MM-IS and MM-MM-Acc algorithms. The recording is performed on a PC with i5-4430 CPU @ 3.00 GHz and 8 GB RAM. Interestingly, the MM-IS algorithm consumes less time than the MM-MM-Acc. It is reasonable since the MM-MM-Acc needs to execute the eigenvalue decomposition to find the largest eigenvalue $\eta_2$ in each iteration.

### 4.2. Sequence Length $N$

In this subsection we assess the performance of **Algorithm 1**[§] for different code sequence lengths. Set the sequence lengths: $N = 2^5, 2^6, 2^7, 2^8, 2^9, 2^{10}$. For all the situations, the stopping criterion is set to $\delta_2 = 10^{-4}$. The random trial number is set to $K = 10$. The statistical average of objective function $\widehat{\mathrm{W}\boldsymbol{\Lambda}}$ is evaluated by

$$\widehat{\mathrm{W}\boldsymbol{\Lambda}} = \frac{1}{K(2N-1)} \sum_{k=1}^{K} \frac{\mathrm{W}\boldsymbol{\Lambda}^{(k)}(\boldsymbol{s}^\star)}{\mathrm{W}\boldsymbol{\Lambda}^{(k)}\left(\boldsymbol{s}^{(0)}\right)}, \tag{17}$$

where $\mathrm{W}\boldsymbol{\Lambda}^{(k)}(\boldsymbol{s}^\star)$ denotes the optimized objective function of the $k$th random trial. Likewise, $\widehat{\mathrm{WICE}}$ and $\widehat{\mathrm{WIASL}}$ are computed by replacing $\mathrm{W}\boldsymbol{\Lambda}^{(k)}(\boldsymbol{s}^\star)$ with $\mathrm{WICE}^{(k)}(\boldsymbol{s}^\star)$ and $\mathrm{WIASL}^{(k)}(\boldsymbol{s}^\star)$, respectively.

In Fig. 2 we plot the statistical objective values of the optimized sequences versus different sequence lengths. Note that these curves are average results over 10 random trials. All $\mathrm{WICE}^{(k)}(\boldsymbol{s}^\star)$, $\mathrm{WIASL}^{(k)}(\boldsymbol{s}^\star)$, and $\widehat{\mathrm{W}\boldsymbol{\Lambda}}$ decrease with the increase of sequence length. WIASL shares a more evident

[§] Due to the approximate convergence optimization tendency of **Algorithm** 1 and **Algorithm** 2 (See Subsection 4.1), we only use the former in following performance analysis.

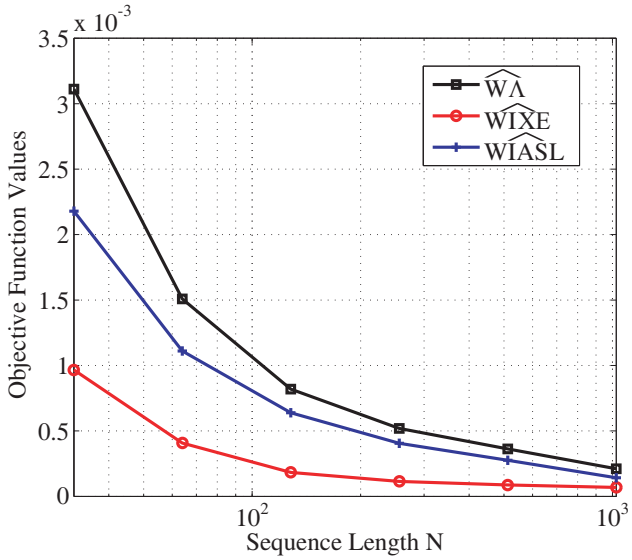


**Figure 2.** Objective function values of the MM-IS sequences for different sequence lengths.

**Table 2.** ASL (dB) and PSL (dB) of ICE and IASL for different sequence lengths.

| N \ Function | AICE | PICE | AIASL | PIASL |
|---|---|---|---|---|
| 64 | −32.37 | −29.89 | −28.26 | −21.34 |
| 256 | −38.19 | −32.35 | −32.62 | −23.13 |

downtrend than WICE, because the real value of WIASL in objective function is larger than WICE when $\lambda = 0.5$. However, this situation can be regulated by weights $\lambda$, $\boldsymbol{w}1$, and $\boldsymbol{w}2$.

Define the cross-correlation (CC) function level and auto-correlation (AC) function level as

$$\mathrm{CC}\,(\mathrm{dB}) = 20\log_{10}\left|\frac{\mathtt{C}_k}{\mathtt{R}_0}\right|, \quad k = -N+1, \ldots, N-1, \tag{18}$$

and

$$\mathrm{AC}\,(\mathrm{dB}) = 20\log_{10}\left|\frac{\mathtt{R}_k}{\mathtt{R}_0}\right|, \quad k = -N+1, \ldots, N-1, \tag{19}$$

respectively, where $\mathtt{C}_k$ and $\mathtt{R}_k$ (See Equations (B1) and (B4)), respectively, denote the auto-correlation and cross-correlation functions at lag $k$.

In Fig. 3, the correlation function curves with different sequence lengths are shown. Table 2 presents the average sidelobe level (ASL) and peak sidelobe level (PSL) of the ICE and IASL for different sequence lengths. It can be observed that the proposed algorithm achieves lower average ICE (AICE) and average IASL (AIASL) when $N = 256$. However, the PSL of ICE (PICE) and PSL of IASL (PIASL) change slowly following the increase of sequence length.

### 4.3. Weights $\lambda$, $w_1$, and $w_2$

In this subsection, the designed sequence length is set to $N = 128$, and the stopping criterion is the same as Subsection 4.2. The statistical $\widetilde{\mathrm{WICE}}$ is computed by

$$\widetilde{\mathrm{WICE}} = \frac{1}{K}\sum_{k=1}^{K}\frac{\mathrm{WICE}^{(k)}(\boldsymbol{s}^\star)}{\mathrm{W}\boldsymbol{\Lambda}^{(k)}(\boldsymbol{s}^\star)}. \tag{20}$$

where $\mathrm{WICE}^{(k)}(\boldsymbol{s}^\star)$ denotes the optimized autocorrelation function of the $k$th random trial. Likewise, $\widetilde{\mathrm{WIASL}}$ is computed by replacing $\mathrm{WICE}^{(k)}(\boldsymbol{s}^\star)$ with $\mathrm{WIASL}^{(k)}(\boldsymbol{s}^\star)$.

In Fig. 4(a), we evaluate the ICE and IASL functions versus different weights $\lambda = [0, 0.1, \ldots, 1]$. Results reveal that the weight $\lambda$ can take a good tradeoff between the ICE and IASL functions. Especially, the change is sensitive when $\lambda$ is close to both the weight ends.

In Fig. 4(b)– 4(c), we show the correlation function level versus $\lambda = 1, 0.5$. Table 3 summarizes the ASL and PSL of ICE and IASL for $\lambda = 1$ and 0.5. It can be observed that both the ASL and PSL of ICE change notably with the adjustment of $\lambda$. Accordingly, an appropriate choice of $\lambda$ becomes more effective and practical than increasing sequence length for obtaining better suppression property.

**Table 3.** ASL (dB) and PSL (dB) of ICE and IASL for Different Weights $\lambda$.

| $\lambda$ \ Function | AICE | PICE | AIASL | PIASL |
|---|---|---|---|---|
| 1 | -39.25 | -34.26 | -25.78 | -16.22 |
| 0.5 | -35.95 | -32.23 | -30.60 | -22.57 |

Besides, we analyze the impact of the weights $\boldsymbol{w}_1$ and $\boldsymbol{w}_2$ on different correlation lag zones. Assume that the weight $\boldsymbol{w}_1$ is given by

$$w_{1,k} = \begin{cases} 1, & k \in [N-30, N+30], \\ 0, & \text{otherwise.} \end{cases} \tag{21}$$

The weight $\boldsymbol{w}_2$ is given by

$$w_{2,k} = \begin{cases} 1, & k \in [1, 30], \\ 0, & \text{otherwise.} \end{cases} \tag{22}$$

In Fig. 5, we provide the correlation function levels of the MM-IS sequence versus lag bin $k$ for weights $\boldsymbol{w}_1$ and $\boldsymbol{w}_2$. We can observe that the ASL and PSL of of ICE in the suppressing zones are $-35.03$ dB and $-31.55$ dB, respectively; the ASL and PSL of IASL in the suppression zones are $-38.69$ dB and $-36.00$ dB, respectively. It is obvious that the sidelobe performance of the suppression zones is better than Fig. 4(c). Hence, we can adjust the weights $\boldsymbol{w}_1$ and $\boldsymbol{w}_2$ to control the distribution of sidelobe energy.

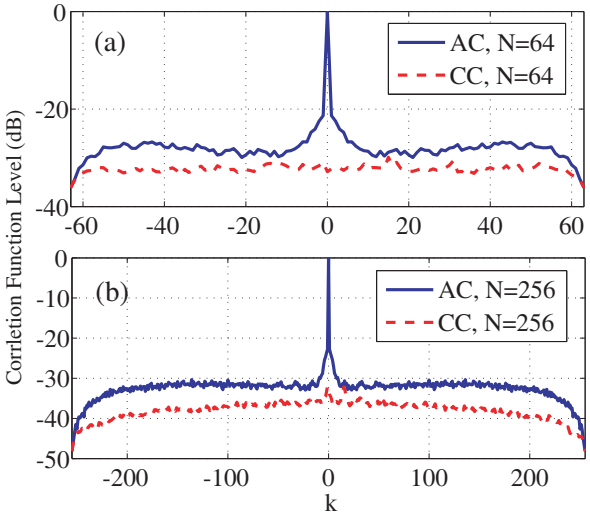


**Figure 3.** Correlation function levels of the MM-IS sequences for different sequence lengths with 100 random trials: (a) $N = 64$ and (b) $N = 256$.

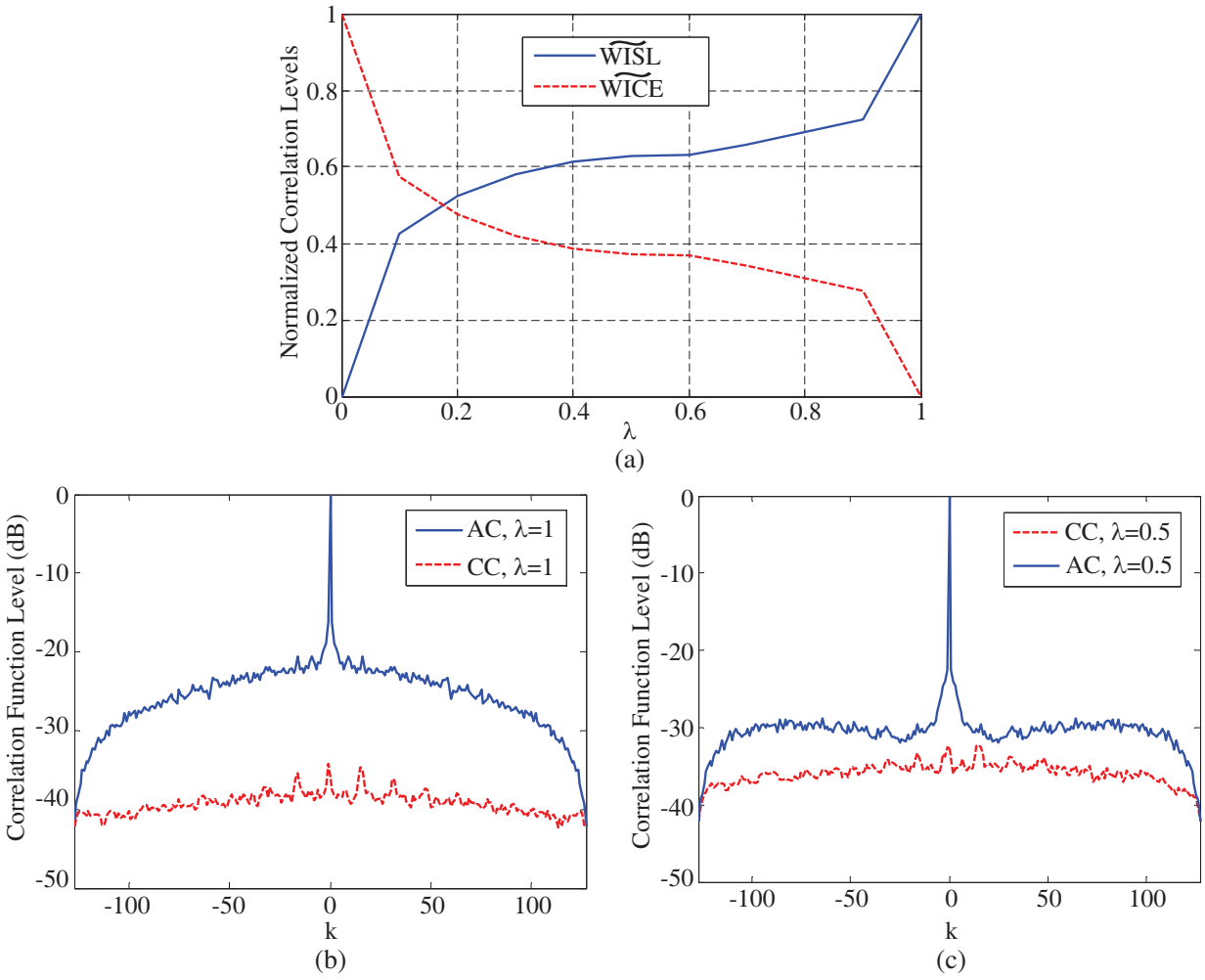


**Figure 4.** Correlation function levels of the MM-IS sequences for (a) different weights $\lambda$ with 10 random trials; (b) $\lambda = 1$ and (c) $\lambda = 0.5$ with 100 random trials.

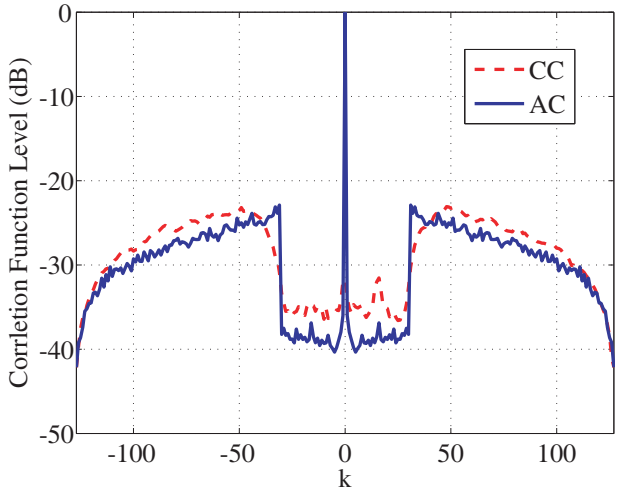


**Figure 5.** Correlation function levels of the MM-IS sequence for given weights $\boldsymbol{w}_1$ and $\boldsymbol{w}_2$ with 100 random trials.

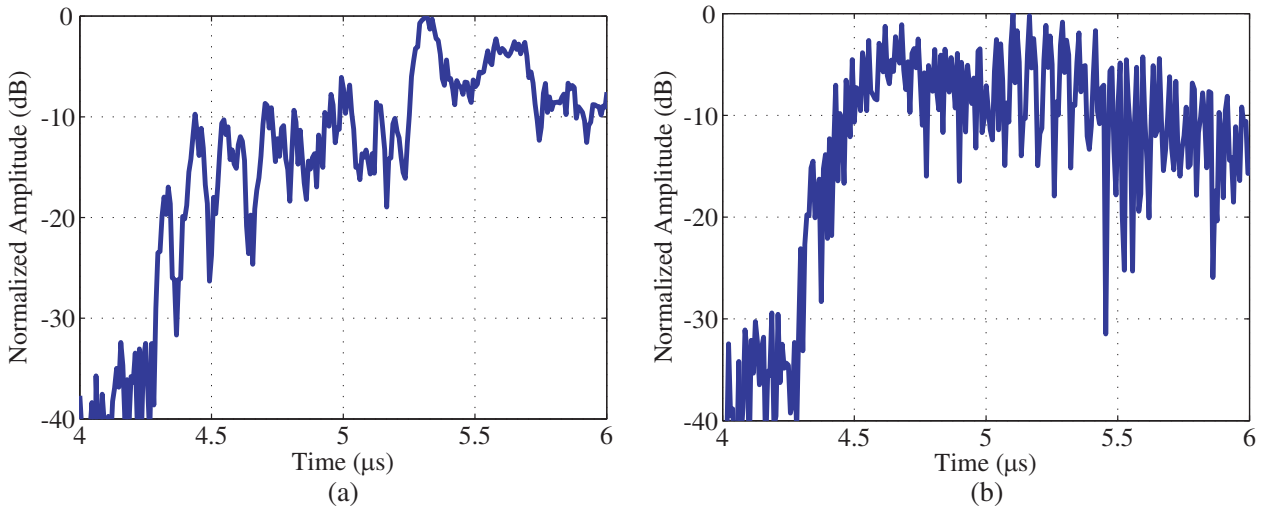


**Figure 6.** The matched filtering results of original sequences for single target and jamming: (a) C&I and (b) SMSP.

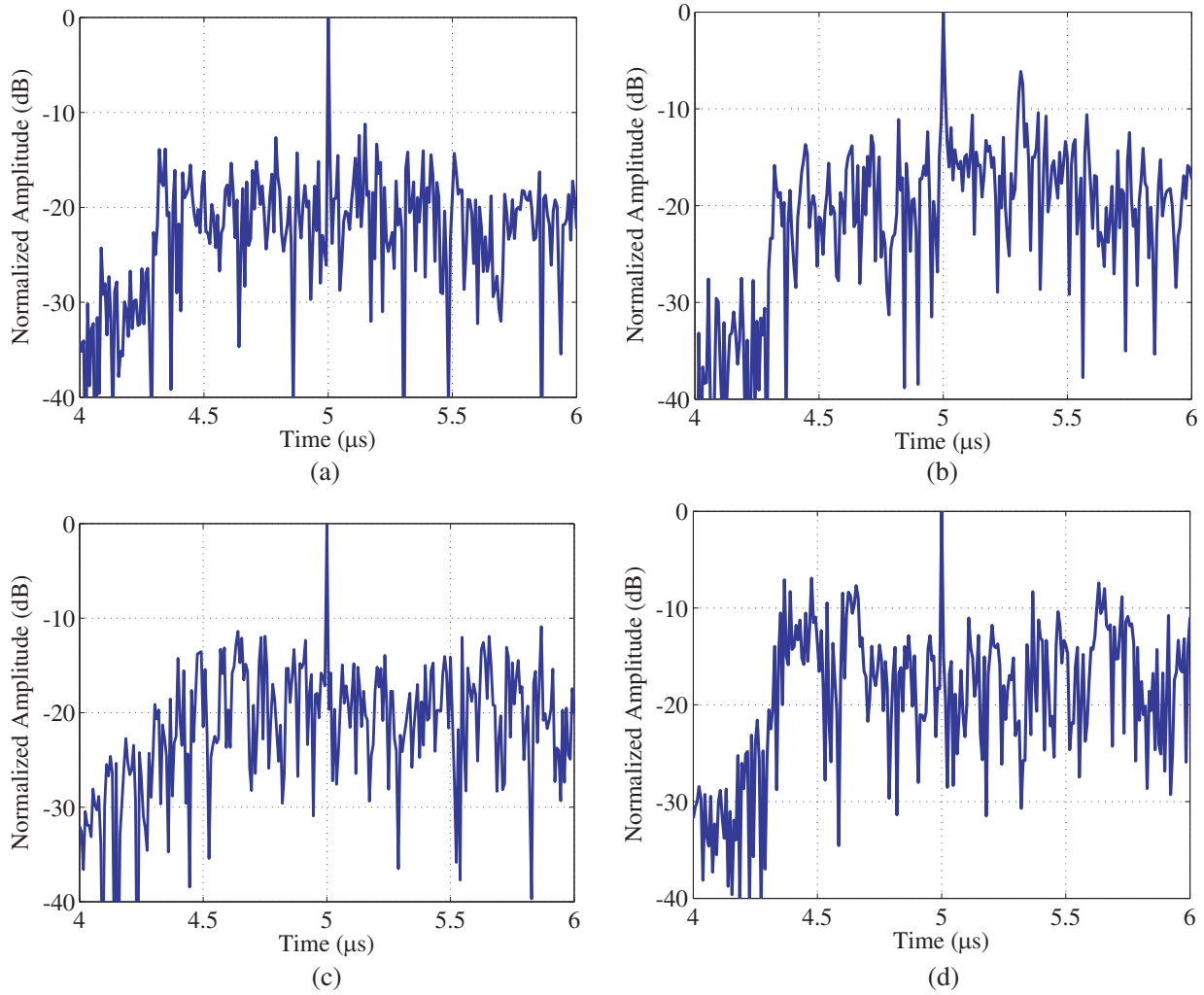


**Figure 7.** The matched filtering results of the optimized sequences for single target and jamming with different weights $\lambda$: (a) C&I, $\lambda = 1$, (b) C&I, $\lambda = 0.5$, (c) SMSP, $\lambda = 1$, and (d) SMSP, $\lambda = 0.5$.

### 4.4. Performance Analysis of Matched-Filter Processing

In this subsection, we provide two kinds of detection scenarios to evaluate the jamming suppression performance of the MM-IS algorithm. After the received signal is down-converted to baseband and sampled in radar receiver, it can be written as

$$\boldsymbol{r} = \alpha_s \boldsymbol{s} + \alpha_c \boldsymbol{c} + \boldsymbol{v}, \tag{23}$$

where $\alpha_s$ denotes the complex amplitude accounting for propagation and backscattering effects from real target, $\alpha_c$ the complex amplitude accounting for propagation effect and additive jamming power, and $\boldsymbol{v}$ the $N$-dimensional column vector of the filtered noise samples assuming that it is a circular complex white Gaussian with zero mean and covariance matrix $\sigma_v^2 \boldsymbol{I}_N$. The output of the discrete-time matched filter with the linear response $\boldsymbol{h}^{(k)} = [s_{1-k}, \ldots, s_{N-k}]^{\dagger}, k = -N+1, \ldots, N-1$, is given by

$$z_k = \boldsymbol{r}^T \boldsymbol{h}^{(k)} = \sum_{n=1}^{N} r_n s_{n-k}*, \quad k = -N+1, \ldots, N-1. \tag{24}$$

In the first scenario, we consider a real target and a strong jamming. Or, a jammer (the real target) retransmits a jamming signal. Set the sequence length $N = 128$, jamming parameters $p = q = 16$ for both C&I and SMSP. The pulse width and pulse repetition time (PRT) are set to 1 μs and 10 μs,

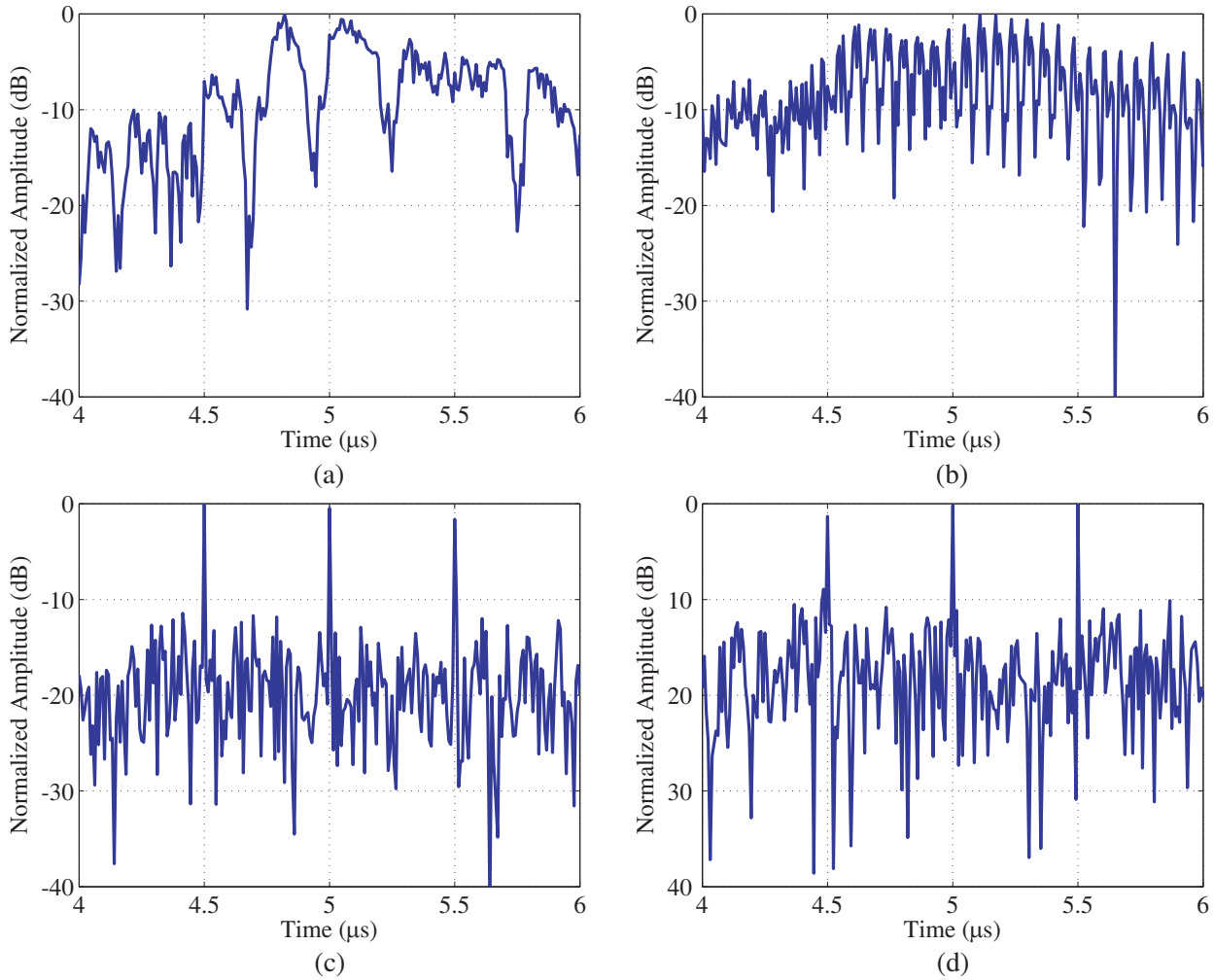


**Figure 8.** The matched filtering results of the original sequences for multiple targets and jammings: (a) C&I and (b) SMSP. The matched filtering results of the optimized sequences with $\lambda = 1$ for multiple targets and jammings: (c) C&I and (d) SMSP.

respectively. The signal to noise ratio (SNR) of the real target and the jamming to signal ratio (JSR) of the jamming are set to 10 dB and 20 dB, respectively. They are located at 5 μs and 5.3 μs, respectively. In other words, the retransmission of the jamming signal lags behind the target echo by 0.3 μs. The Monte-Carlo number of the matched filtering process aiming at random noise is 200.

In Fig. 6, we show the matched filtering results of unoptimized transmit sequences for single target and jamming with different weights $\lambda$. It can be observed that the true targets are hard to be detected accurately in Fig. 6 due to the strong adjacent interference. Besides, many false peak range cells can be detected. In Fig. 7, we show the matched filtering results using the optimized code sequences. The PSLs of Fig. 7(a)–7(d) are −11.63 dB, −6.04 dB, −11.18 dB, and −7.03 dB, respectively. The peak values of real targets are about 11 dB higher than PSL when $\lambda = 1$. Obviously, the real targets are easy to be detected, and the false targets are also suppressed. The performance of jamming suppression for $\lambda = 1$ is better than $\lambda = 0.5$.

In the second scenario, there are three jammers with the same jamming forms. They are located at 4.5 μs, 5 μs, and 5.5 μs, respectively. All the jamming delays of three jammers are behind the targets by 0.3 μs. The other parameters are set the same as the first scene. Figs. 8(a)–8(b) show the matched filtering results of original sequences, where many false targets can be detected, but three real targets are drowned. Fig. 8(c) shows the result of the optimized code sequence for C&I jamming. The neighboring PSLs of three real targets are −12.04 dB, −11.65 dB, and −10.42 dB. Fig. 8(d) shows the result of the optimized code sequence for SMSP jamming. The neighboring PSLs of three real targets are −9.57 dB, −11.39 dB, and −10.05 dB. The jamming suppression performance is very close to the first scenario. Overall, multiple jammings are suppressed well, and all real targets are easy to be detected. It is worth noting that the used optimized sequences for C&I (or SMSP) jammings in the first and second scenarios are the same. Therefore, for a certain jamming form, the sequence only needs to be optimized once whatever there may be one or multiple targets and jammings, and whatever the jamming delay changes.

## 5. CONCLUSIONS

In this paper, we have addressed the problem of cognitive waveform design in the presence of signal-dependent modulated jamming. Our main conclusions are summarized as follows:

- We have generalized some signal-dependent modulated jammings into a common form $\boldsymbol{c} = \boldsymbol{J}_c\boldsymbol{s}$. The minimization of the cross-correlation energy between transmit signal and jamming is taken as a criterion of jamming rejection. Meanwhile, low IASL of transmit signal is also considered. Finally, we formulate and convert the waveform design problem into a unified simplified model $\boldsymbol{s}^\dagger\boldsymbol{\Phi}(\boldsymbol{s})\boldsymbol{s}$.
- We have proposed an iterative optimization algorithm to solve the waveform design problem. Firstly, the objective function related to the fourth power of transmit waveform is translated into the quadratic form $\boldsymbol{s}^\dagger\boldsymbol{\Upsilon}\boldsymbol{s}$. It is a classical unimodular quadratic program problem. Some devised optimization algorithms such as SDP can be used. Secondly, we have introduced the iteration search method based on alternate optimization of each code element to solve the quadratic program problem.
- We have accessed the MM-IS algorithm through numerical simulations. The results indicate that the whole performance can be improved as sequence length increases. The weight $\lambda$ can trade off between ICE and IASL. Besides, the weights $\boldsymbol{w}_1$ and $\boldsymbol{w}_2$ can regulate the suppression of different range cells. Moreover, the sequence only needs to be optimized once for one or multiple certain jammings with changed delay.

In order to better cope with the changing jamming environment, in the future we might research on improving the iteration convergence speed [36]. Another potential future work is to extend this paper to a co-located MIMO radar system [37].

## ACKNOWLEDGMENT

This work was supported by the National Natural Science Foundation of China under Grants 61771109 and 61501083, the Fundamental Research Funds of Central Universities under Grants ZYGX2013J012, the Chinese Postdoctoral Science Foundation under Grant 2014M550465 and Specail Grant 2016T90845.

## APPENDIX A. MODULATION TYPES OF C&I AND SMSP

With reference to the generation mechanism of the C&I jamming [20], the modulation of C&I jamming for the transmit signal $\boldsymbol{s}$ contains two steps. First, the jammer samples the intercepted radar signal $\boldsymbol{s}$ at regular intervals. Second, it replicates the samples in turn in the adjacent intervals until filling the interval spaces up. The jamming signal $\boldsymbol{ci}$ can be written as

$$\boldsymbol{c}i = \frac{1}{\sqrt{N}}\left[e^{j\boldsymbol{\phi}_1}, \ldots, e^{j\boldsymbol{\phi}_1}, \ldots, e^{j\boldsymbol{\phi}_{(l-1)p+1}}, \ldots, e^{j\boldsymbol{\phi}_{(l-1)p+1}}\right]^T$$

where $p$ and $l$ denote the repetition times of each sample and the total sample number of C&I jamming, respectively. Besides, the sequence length meets $N = pl$. Accordingly the C&I jamming shifting matrix $\boldsymbol{J}_{ci}$ is given by

$$\boldsymbol{J}_{ci} = \begin{bmatrix} \overbrace{1\,0\ldots0}^{p} & & 0 \\ \vdots & & \\ 1\,0\ldots0 & & \\ & \ddots & \\ & & 1\,0\ldots0 \\ & & \vdots \\ 0 & & 1\,0\ldots0 \end{bmatrix}_{N\times N} \tag{A1}$$

Likewise, the SMSP jamming signal $\boldsymbol{sm}$ also contains two steps. The first step is the same as the C&I jamming. In the second step, it compresses all the samples and replicates them in the subsequent intervals until filling the interval spaces up. The jamming signal $\boldsymbol{sm}$ can be written as

$$\boldsymbol{sm} = \frac{1}{\sqrt{N}}\left[\underbrace{e^{j\boldsymbol{\phi}_1}, e^{j\boldsymbol{\phi}_{q+1}}, \ldots, e^{j\boldsymbol{\phi}_{N-q+1}}}_{L}, \ldots, e^{j\boldsymbol{\phi}_1}, e^{j\boldsymbol{\phi}_{q+1}}, \ldots, e^{j\boldsymbol{\phi}_{N-q+1}}\right]^T$$

where $q$ and $L$ denote the repetition times of each sample and the total sample number of the SMSP jamming, respectively, and $N = qL$. $\boldsymbol{J}_{sm}$ can be written as

$$\boldsymbol{J}_{sm} = \begin{bmatrix} \overbrace{1\,0\ldots0}^{q} & & & 0 \\ & 1\,0\ldots0 & & \\ & & \ddots & \\ & & & 1\,0\ldots0 \\ & \vdots & & \\ 1\,0\ldots0 & & & \\ & 1\,0\ldots0 & & \\ & & \ddots & \\ 0 & & & 1\,0\ldots0 \end{bmatrix}_{N\times N} \tag{A2}$$

## APPENDIX B. PROOF OF PROPOSITION 2.1

The cross-correlation function of the transmit signal $\boldsymbol{s}$ and jamming signal $\boldsymbol{c}$ at lag $k$ is defined as

$$\mathtt{C}_k = \begin{cases} \sum_{n=1}^{N-k} c_{n+k} s_n *, & k = 0, \ldots, N-1, \\ \sum_{n=1}^{N+k} c_n s_{n-k} *, & k = -N+1, \ldots, -1. \end{cases} \tag{B1}$$

Set the following "shifting matrix":

$$\boldsymbol{J}_k = \begin{bmatrix} \overbrace{0\ldots0}^{k} & 1 & & 0 \\ & & \ddots & \\ & & & 1 \\ 0 & & & \end{bmatrix}_{N\times N}, \quad k = 0, \ldots, N-1. \tag{B2}$$

Under the assumption that the shifting matrix of the signal-dependent interference $\boldsymbol{c}$ in Equation (2) is known, Eq. (B1) can be rewritten as

$$\mathtt{C}_k = \begin{cases} \boldsymbol{s}^\dagger \boldsymbol{J}_k \boldsymbol{J}_c \boldsymbol{s}, & k = 0, \ldots, N-1, \\ \boldsymbol{s}^\dagger \boldsymbol{J}_{-k}^T \boldsymbol{J}_c \boldsymbol{s}, & k = -N+1, \ldots, -1. \end{cases}$$

The integrated cross-correlation energy function at lag $k$ is given by

$$\mathrm{ICE}(\boldsymbol{s}) = \sum_{k=-N+1}^{N-1} |\mathtt{C}_k|^2 = \sum_{k=1}^{N-1} \left| \boldsymbol{s}^\dagger \boldsymbol{J}_k^T \boldsymbol{J}_c \boldsymbol{s} \right|^2 + \sum_{k=0}^{N-1} \left| \boldsymbol{s}^\dagger \boldsymbol{J}_k \boldsymbol{J}_c \boldsymbol{s} \right|^2. \tag{B3}$$

For the transmit signal $\boldsymbol{s}$, its aperiodic auto-correlation function is defined as

$$\mathtt{R}_k = \begin{cases} \displaystyle\sum_{n=1}^{N-k} s_{n+k} s_n^*, & k = 0, \ldots, N-1, \\ \displaystyle\sum_{n=1}^{N+k} s_n s_{n-k}^*, & k = -N+1, \ldots, -1. \end{cases} \tag{B4}$$

Similarly, using the shifting matrix $\boldsymbol{J}_k$, Eq. (B4) can be rewritten as

$$\mathtt{R}_k = \begin{cases} \boldsymbol{s}^\dagger \boldsymbol{J}_k \boldsymbol{s}, & k = 0, \ldots, N-1, \\ \boldsymbol{s}^\dagger \boldsymbol{J}_{-k}^T \boldsymbol{s}, & k = -N+1, \ldots, -1. \end{cases} \tag{B5}$$

It can be easily proved that $\mathtt{R}_k = \mathtt{R}_{-k}*$. Then the IASL function is defined as

$$\mathrm{IASL}(\boldsymbol{s}) = \sum_{k=-N+1,\ k\neq 0}^{N-1} |\mathtt{R}_k|^2 = 2\sum_{k=1}^{N-1} \left| \boldsymbol{s}^\dagger \boldsymbol{J}_k \boldsymbol{s} \right|^2. \tag{B6}$$

## APPENDIX C. PROOF OF PROPOSITION 3.1

Let $\boldsymbol{S} = \boldsymbol{s}\boldsymbol{s}^\dagger \in \mathbb{C}^{N\times N}$. With reference to Eq. (7), the first term of WICE can be recast as

$$\begin{aligned} \lambda \sum_{k=1}^{N-1} w_{1,N-k} \left| \boldsymbol{s}^\dagger \boldsymbol{J}_k^T \boldsymbol{J}_c \boldsymbol{s} \right|^2 &= \lambda \sum_{k=1}^{N-1} w_{1,N-k} \left| \mathrm{Tr}\left( \boldsymbol{S} \boldsymbol{J}_k^T \boldsymbol{J}_c \right) \right|^2 \\ &= \lambda \sum_{k=1}^{N-1} w_{1,N-k} \left| \mathrm{vec}(\boldsymbol{S})^\dagger \mathrm{vec}(\boldsymbol{J}_k^T \boldsymbol{J}_c) \right|^2 \\ &= \mathrm{vec}(\boldsymbol{S})^\dagger \left[ \lambda \sum_{k=1}^{N-1} w_{1,N-k} \mathrm{vec}(\boldsymbol{J}_k^T \boldsymbol{J}_c) \mathrm{vec}(\boldsymbol{J}_k^T \boldsymbol{J}_c)^\dagger \right] \mathrm{vec}(\boldsymbol{S}). \end{aligned}$$

Likewise, the objective function $\mathrm{W}\boldsymbol{\Lambda}(\boldsymbol{s}, \lambda, \boldsymbol{w}_1, \boldsymbol{w}_2)$ can be rewritten as

$$\mathrm{W}\boldsymbol{\Lambda}(\boldsymbol{s}, \lambda, \boldsymbol{w}_1, \boldsymbol{w}_2) = \mathrm{vec}(\boldsymbol{S})^\dagger \left( \boldsymbol{\Psi}_1 + \boldsymbol{\Psi}_2 + \boldsymbol{\Psi}_3 \right) \mathrm{vec}(\boldsymbol{S}) = \mathrm{vec}(\boldsymbol{S})^\dagger \boldsymbol{\Psi} \mathrm{vec}(\boldsymbol{S}), \tag{C1}$$

where

$$\begin{cases} \boldsymbol{\Psi}_1 = \lambda \sum_{k=1}^{N-1} w_{1,N-k} \mathrm{vec}(\boldsymbol{J}_k^T \boldsymbol{J}_c) \mathrm{vec}(\boldsymbol{J}_k^T \boldsymbol{J}_c)^\dagger \\ \boldsymbol{\Psi}_2 = \lambda \sum_{k=0}^{N-1} w_{1,N+k} \mathrm{vec}(\boldsymbol{J}_k \boldsymbol{J}_c) \mathrm{vec}(\boldsymbol{J}_k \boldsymbol{J}_c)^\dagger \\ \boldsymbol{\Psi}_3 = 2(1-\lambda) \sum_{k=1}^{N-1} w_{2,k} \mathrm{vec}(\boldsymbol{J}_k) \mathrm{vec}(\boldsymbol{J}_k)^\dagger \end{cases} \tag{C2}$$

and $\boldsymbol{\Psi}_i^\dagger = \boldsymbol{\Psi}_i,\ i = 1, 2, 3.$

Let

$$\boldsymbol{M} = \lambda_{\max} \boldsymbol{I}_N,$$

where $\lambda_{\max}$ is the maximum eigenvalue of the matrix $\boldsymbol{\Psi}$. Here we would highlight the solving approach of $\lambda_{\max}$. Due to $\boldsymbol{J}_k, \boldsymbol{J}_c \in \mathbb{C}^{N\times N}$, $\boldsymbol{\Psi} \in \mathbb{C}^{NN\times NN}$, it is very time-consuming to solve $\lambda_{\max}$ when $N$ is large. We notice that $\boldsymbol{J}_k, \boldsymbol{J}_c$, and $\boldsymbol{\Psi}$ are greatly sparse, especially the last one, $\boldsymbol{\Psi}$. So we take the sparse processing for the related matrixes as much as possible. in this process. The running time is greatly reduced.

According to Lemma 1 in [24], the majorization function of Eq. (C1) is constructed by the following equation at $\boldsymbol{S}^{(m)}$:

$$\begin{aligned} u_1\left(\boldsymbol{S}, \boldsymbol{S}^{(m)}\right) &= \lambda_{\max} \mathrm{vec}(\boldsymbol{S})^\dagger \mathrm{vec}(\boldsymbol{S}) + \mathrm{vec}\left(\boldsymbol{S}^{(m)}\right)^\dagger (\boldsymbol{M} - \boldsymbol{\Psi}) \mathrm{vec}\left(\boldsymbol{S}^{(m)}\right) \\ &\quad + 2\Re e\left(\mathrm{vec}(\boldsymbol{S})^\dagger (\boldsymbol{\Psi} - \boldsymbol{M}) \mathrm{vec}\left(\boldsymbol{S}^{(m)}\right)\right), \end{aligned} \tag{C3}$$

where $m$ denotes the $m$th iteration. Obviously, $\mathrm{vec}(\boldsymbol{S})^\dagger \mathrm{vec}(\boldsymbol{S}) = (\boldsymbol{s}^\dagger \boldsymbol{s})^2 = 1$, and $\boldsymbol{S}^{(m)}$ is a constant relative to $\boldsymbol{S}$. Ignoring the constant terms, the majorized problem is given by

$$\begin{aligned} \min_{\boldsymbol{s}} \quad & \Re e\left(\mathrm{vec}(\boldsymbol{S})^\dagger (\boldsymbol{\Psi} - \boldsymbol{M}) \mathrm{vec}(\boldsymbol{S}^{(m)})\right) \\ \text{s.t.} \quad & \boldsymbol{S} = \boldsymbol{s}\boldsymbol{s}^\dagger, \\ & |s_n| = \frac{1}{\sqrt{N}}, \quad n = 1, \ldots, N. \end{aligned} \tag{C4}$$

Let us define $g = \mathrm{vec}(\boldsymbol{S})^\dagger (\boldsymbol{\Psi} - \boldsymbol{M}) \mathrm{vec}(\boldsymbol{S}^{(m)})$. Then the majorized objective function of Eq. (C4) can be rewritten as

$$\Re e\left(\mathrm{vec}(\boldsymbol{S})^\dagger (\boldsymbol{\Psi} - \boldsymbol{M}) \mathrm{vec}\left(\boldsymbol{S}^{(m)}\right)\right) = \frac{g + g^\dagger}{2}, \tag{C5}$$

where $g^\dagger$ is computed by Equations (C6) and (C7).

$$\begin{aligned} g^\dagger &= \mathrm{vec}\left(\boldsymbol{S}^{(m)}\right)^\dagger (\boldsymbol{\Psi} - \boldsymbol{M}) \mathrm{vec}(\boldsymbol{S}) \\ &= \mathrm{vec}\left(\boldsymbol{S}^{(m)}\right)^\dagger \left\{ \lambda \Big[ \sum_{k=1}^{N-1} w_{1,N-k} \mathrm{vec}(\boldsymbol{J}_k^T \boldsymbol{J}_c) \mathrm{vec}(\boldsymbol{J}_k^T \boldsymbol{J}_c)^\dagger + \sum_{k=0}^{N-1} w_{1,N+k} \mathrm{vec}(\boldsymbol{J}_k \boldsymbol{J}_c) \mathrm{vec}(\boldsymbol{J}_k \boldsymbol{J}_c)^\dagger \Big] \right. \\ &\quad \left. + 2(1-\lambda) \sum_{k=1}^{N-1} w_{2,k} \mathrm{vec}(\boldsymbol{J}_k) \mathrm{vec}(\boldsymbol{J}_k)^\dagger \right\} \mathrm{vec}(\boldsymbol{S}) - \lambda_{\max} \mathrm{Tr}\left(\boldsymbol{S}^{(m)} \boldsymbol{S}\right) \\ &= \lambda \Big[ \sum_{k=1}^{N-1} w_{1,N-k} (\boldsymbol{s}^{(m)})^\dagger \boldsymbol{J}_k^T \boldsymbol{J}_c \boldsymbol{s}^{(m)} \boldsymbol{s}^\dagger (\boldsymbol{J}_k^T \boldsymbol{J}_c)^\dagger \boldsymbol{s} + \sum_{k=0}^{N-1} w_{1,N+k} \left(\boldsymbol{s}^{(m)}\right)^\dagger \boldsymbol{J}_k \boldsymbol{J}_c \boldsymbol{s}^{(m)} \boldsymbol{s}^\dagger (\boldsymbol{J}_k \boldsymbol{J}_c)^\dagger \boldsymbol{s} \Big] \\ &\quad + 2(1-\lambda) \sum_{k=1}^{N-1} w_{2,k} \left(\boldsymbol{s}^{(m)}\right)^\dagger \boldsymbol{J}_k \boldsymbol{s}^{(m)} \boldsymbol{s}^\dagger \boldsymbol{J}_k^T \boldsymbol{s} - \lambda_{\max} \boldsymbol{s}^\dagger \left( \boldsymbol{s}^{(m)} \left(\boldsymbol{s}^{(m)}\right)^\dagger \right) \boldsymbol{s} \\ &= \boldsymbol{s}^\dagger \boldsymbol{G}\left(\boldsymbol{s}^{(m)}\right) \boldsymbol{s} \end{aligned} \tag{C6}$$

where

$$\mathbf{G}\left(\boldsymbol{s}^{(m)}\right) = \sum_{k=1}^{N-1}\left\{\lambda\left[w_{1,N-k}(\boldsymbol{s}^{(m)})^{\dagger}\boldsymbol{J}_k^T\boldsymbol{J}_c\boldsymbol{s}^{(m)}\boldsymbol{J}_c^{\dagger}\boldsymbol{J}_k + w_{1,N+k}\left(\boldsymbol{s}^{(m)}\right)^{\dagger}\boldsymbol{J}_k\boldsymbol{J}_c\boldsymbol{s}^{(m)}\boldsymbol{J}_c^{\dagger}\boldsymbol{J}_k^T\right]\right.$$
$$\left.+2(1-\lambda)w_{2,k}(\boldsymbol{s}^{(m)})^{\dagger}\boldsymbol{J}_k\boldsymbol{s}^{(m)}\boldsymbol{J}_k^T\right\}+\lambda w_{1,N}\left(\boldsymbol{s}^{(m)}\right)^{\dagger}\boldsymbol{J}_c\boldsymbol{s}^{(m)}\boldsymbol{J}_c^{\dagger}-\lambda_{\max}\left(\boldsymbol{s}^{(m)}\left(\boldsymbol{s}^{(m)}\right)^{\dagger}\right). \quad \text{(C7)}$$

Thereby the objective function of Eq. (C4) can be recast as

$$\frac{g+g^{\dagger}}{2} = \frac{\boldsymbol{s}^{\dagger}\boldsymbol{G}^{\dagger}\boldsymbol{s}+\boldsymbol{s}^{\dagger}\boldsymbol{G}\boldsymbol{s}}{2} = \boldsymbol{s}^{\dagger}\boldsymbol{\Upsilon}\left(\boldsymbol{s}^{(m)}\right)\boldsymbol{s}. \quad \text{(C8)}$$

## REFERENCES


1. Kong, L. and M. Luo, "Co-frequency interference suppression algorithm via maximum signal minus interference level," *Progress In Electromagnetics Research*, Vol. 104, No. 4, 183–199, 2010.
2. Kleeman, L., "Real time mobile robot sonar with interference rejection," *Sensor Review*, Vol. 19, No. 3, 214–221, 1999.
3. Zhou, L. L., H. B. Zhu, and N. T. Zhang, "Iterative solution to the notched waveform design in cognitive ultra-wideband radio system," *Progress In Electromagnetics Research*, Vol. 75, 271–284, 2007.
4. Aubry, A., A. De Maio, A. Farina, et al., "Knowledge-aided (potentially cognitive) transmit signal and receive filter design in signal-dependent clutter," *IEEE Transactions on Aerospace and Electronic Systems*, Vol. 49, No. 1, 93–117, 2013.
5. Li, N. and Y. Zhang, "a survey of radar ECM and ECCM," *IEEE Transactions on Aerospace and Electronic Systems*, Vol. 31, No. 3, 1110–1120, 1995.
6. Van Trees, H. L., "Optimum signal design and processing for reverberation-limited environments," *IEEE Transactions on Military Electronics*, Vol. 9, No. 3, 212–229, 1965.
7. Lu, S., G. Cui, W. Yi, et al., "Radar waveform design against signal-dependent jamming," *IEEE Radar Conference*, 1075–1080, 2017.
8. Fu, Y., G. Cui, and X. Yu, "Robust design of constant modulus sequence and receiver filter in the presence of signal-dependent clutter," *Journal of Radars*, Vol. 6, No. 3, 292–299, 2017.
9. Stoica, P., J. Li, and Y. Xie, "On probing signal design for MIMO radar," *IEEE Transactions on Signal Processing*, Vol. 55, No. 8, 4151–4161, 2007.
10. Li, J., J. R. Guerci, and L. Xu, "Signal waveform's optimal under restriction design for active sensing," *In Fourth IEEE Workshop on Sensor Array and Multichannel Processing*, 382–386, 2006.
11. De Maio, A., S. De Nicola, Y. Huang, et al., "Design of phase codes for radar performance optimization with a similarity constraint," *IEEE Transactions on Signal Processing*, Vol. 57, No. 2, 610–621, 2009.
12. Cui, G., Y. Fu, X. Yu, et al., "Local ambiguity function shaping via unimodular sequence design," *IEEE Signal Processing Letters*, Vol. 24, No. 7, 977–981, 2017.
13. Stoica, P., J. Li, and M. Xue, "Transmit codes and receive filters for radar," *IEEE Signal Processing Magazine*, Vol. 25, No. 6, 94–109, 2008.
14. Chen, C. Y. and P. P. Vaidyanathan, "MIMO radar waveform optimization with prior information of the extended target and clutter," *IEEE Transactions on Signal Processing*, Vol. 57, No. 9, 3533–3544, 2009.
15. Romero, R. A. and N. A. Goodman, "Waveform design in signal-dependent interference and application to target recognition with multiple transmissions," *IET Radar, Sonar & Navigation*, Vol. 3, No. 4, 328–340, 2009.
16. Stoica, P., H. He, and J. Li, "Optimization of the receive filter and transmit sequence for active sensing," *IEEE Transactions on Signal Processing*, Vol. 60, No. 4, 1730–1740, 2012.

17. Aubry, A., A. De Maio, M. Piezzo, et al., "Cognitive design of the receive filter and transmitted phase code in reverberating environment," *IET Radar, Sonar & Navigation*, Vol. 6, No. 9, 822–833, 2012.
18. Cui, G., H. Li, and M. Rangaswamy, "MIMO radar waveform design with constant modulus and similarity constraints," *IEEE Transactions on Signal Processing*, Vol. 62, No. 2, 343–353, 2014.
19. Tang, B., J. Li, Y. Zhang, et al., "Design of MIMO radar waveform covariance matrix for Clutter and Jamming suppression based on space time adaptive processing," *Signal Processing*, Vol. 121, 60–69, 2016.
20. Sparrow, M. J. and J. Cikalo, "ECM techniques to counter pulse compression radar," U.S. Patent, No. 7,081,846, 2006.
21. Lu, S., W. Yi, G. Cui, et al., "Design and application of dynamic environmental knowledge base," *IET Radar, Sonar & Navigation*, Vol. 10, No. 6, 1118–1126, 2016.
22. Aubry, A., A. De Maio, M. Piezzo, et al., "Cognitive radar waveform design for spectral coexistence in signal-dependent interference," *IEEE Radar Conference*, 0474–0478, 2013.
23. Wang, G. and Y. L. Lu, "Sparse frequency waveform design for MIMO radar," *Progress In Electromagnetics Research B*, Vol. 20, 19–32, 2010.
24. Song, J., P. Babu, and D. P. Palomar, "Optimization methods for designing sequences with low autocorrelation sidelobes," *IEEE Transactions on Signal Processing*, Vol. 63, No. 15, 3998–4009, 2015.
25. Haykin, S., "Cognitive radar: A way of the future," *IEEE Signal Processing Magazine*, Vol. 23, No. 1, 30–40, 2006.
26. Zeng, D., H. Xiong, J. Wang, and B. Tang, "An approach to intra-pulse modulation recognition based on the ambiguity function," *Circuits, Systems and Signal Processing*, Vol. 29, No. 6, 1103–1122, 2010.
27. Greco, M., F. Gini, and A. Farina, "Radar detection and classification of jamming signals belonging to a cone class," *IEEE Transactions on Signal Processing*, Vol. 56, No. 5, 1984–1993, 2008.
28. Li, Y., Y. Xiong, and B. Tang, "SMSP jamming identification based on Matched Signal transform," *2011 IEEE International Conference on Computational Problem-Solving (ICCP)*, 182–185, 2011.
29. Zhou, C., F. Shi, and Q. Liu, "Research on parameters estimation and suppression for C&I jamming," *2016 CIE International Conference on Radar*, 1–4, 2016.
30. Boyd, S. and L. Vandenberghe, *Convex Optimization*, Cambridge University Press, 2004.
31. Zhang, S. and Y. Huang, "Complex quadratic optimization and semidefinite programming," *SIAM J. Optimiz.*, Vol. 16, No. 3, 871–890, 2006.
32. Soltanalian, M. and P. Stoica, "Designing unimodular codes via quadratic optimization," *IEEE Transactions on Signal Processing*, Vol. 62, No. 5, 1221–1234, 2014.
33. Hunter, D. R. and K. Lange, "A tutorial on MM algorithms," *The American Statistician*, Vol. 58, No. 1, 30–37, 2004.
34. Stoica, P. and Y. Selen, "Cyclic minimizers, majorization techniques, and the expectation-maximization algorithm: A refresher," *IEEE Signal Processing Magazine*, Vol. 21, No. 1, 112–114, 2004.
35. Cui, G., X. Yu, G. Foglia, et al., "Quadratic optimization with similarity constraint for unimodular sequence synthesis," *IEEE Transactions on Signal Processing*, Vol. 65, No. 18, 4756–4769, 2017.
36. Varadhan, R. and C. Roland, "Simple and globally convergent methods for accelerating the convergence of any EM algorithm," *Scandinavian Journal of Statistics*, Vol. 35, No. 2, 335–353, 2008.
37. Cui, G., X. Yu, V. Carotenuto, et al., "Space-time transmit code and receive filter design for colocated MIMO Radar," *IEEE Transactions on Signal Processing*, Vol. 65, No. 5, 1116–1129, 2017.